

Relaxor Properties of $(\text{Pb}_{0.75}\text{Ba}_{0.25})(\text{Zr}_{0.70}\text{Ti}_{0.30})\text{O}_3$ Ceramics

Z. Ujma,* M. Adamczyk and J. Hańderek

Institute of Physics, University of Silesia, Katowice, Poland

(Received 3 February 1998; accepted 16 June 1998)

Abstract

Dielectric constant and loss factor were investigated as a function of temperature for different frequencies of the measuring field for the $(\text{Pb}_{0.75}\text{Ba}_{0.25})(\text{Zr}_{0.70}\text{Ti}_{0.30})\text{O}_3$ ceramics. Additional measurements of the pyroelectric and thermally stimulated depolarization currents were carried out. The results obtained show distinct correlation. They also prove that these ceramics show properties of relaxor ferroelectrics. © 1998 Elsevier Science Limited. All rights reserved

1 Introduction

Structural studies of the system $(\text{Pb,Ba})(\text{Zr,Ti})\text{O}_3$, (PBZT) were performed by Ikeda¹ who worked out the phase diagram on this base. Dielectric measurements show that an increase of Ba concentration in the ceramics with constant Zr/Ti ratios results in decrease of temperature T_m corresponding to the broad maximum in the curve of dielectric constant (ϵ) versus temperature.

The solid solutions containing about 25–35 at% of Ba have relatively high ϵ and low dielectric losses ($\tan \delta$). The dielectric and other measurements for the PBZT system were repeated recently by Li and Haertling.² Relaxor behaviour was found in the ceramics for the range of compositions near the boundaries between the ferroelectric (FE) rhombohedral, tetragonal and paraelectric (PE) cubic phases. Characteristic of the ferroelectric relaxors slim hysteresis loops and frequency dependence of $\epsilon(T)$ curves were identified for the ceramics of these compositions.

Apparently the ferroelectric relaxors of quick response have already found many applications

and further potential applications can be expected. For instance, owing to the utilization of the peculiar relaxor properties of some $(\text{Pb,L a})(\text{Zr,Ti})\text{O}_3$, (PLZT) ceramics and the fast rising short high-voltage impulses, the exceptional strong electron emission was discovered.^{3–5} The coexistence of neighbouring phases in the regions of diffuse FE–PE and AFE–FE phase transitions and the occurrence of quick switchable FE microdomains play an important role in this process.

As shown in Ref. 2, the PBZT ceramics of the composition 25–35/70/30 (Ba/Zr/Ti) belong to the relaxor phase region. Dielectric properties of these ceramics were also investigated recently by Kanai *et al.*⁶ It is reasonable to believe that these ceramics can be useful as the electron emitters, similarly as the PLZT ceramics mentioned above. To prepare samples of the PBZT ceramics for the experiments with electrically and optically stimulated electron emission the dielectric and pyroelectric properties of these ceramics were examined in order to learn how they behave as relaxors. The results obtained for one of the studied materials namely that of composition 25/70/30 are reported in the present paper as an example.

2 Sample Preparation

The PBZT ceramics of composition 25/70/30 was prepared using conventional mixed-oxide processing technique. The proper amounts of reagents: PbO , BaCO_3 , TiO_2 and ZrO_2 were weighed and blended. Thermal synthesis of the pressed oxides was carried out at 925°C in 2 h. The crumbled, milled and sieved material was pressed again in the form of cylinders and then sintered at 1250°C in 4 h. This procedure was repeated before the final sintering at 1300°C in 7 h. These sintering processes were carried out as follows: the material was placed in a double crucible with some amount of PbO and ZrO_2 , in order to maintain the established

*To whom correspondence should be addressed. Fax: +48-32-588431; e-mail: ujma@us.edu.pl

composition, and especially to avoid the loss of PbO caused by its sublimation.

The scanning electron microscope JSM-5410 with an energy dispersive X-ray spectrometer (EDS) was used for investigation of the grain structure and composition of the obtained ceramics. A typical scanning electron micrograph of fracture surface of the investigated PBZT-25/70/30 ceramics is shown in Fig. 1(a). The average grain size was of the order of 15 micron. Porosity of this ceramics was relatively high because, unlike other authors² we did not use admixtures like Bi₂O₃, known for improving sinterability and microstructure of PBZT ceramics. The example of EDS analysis, obtained for one of the grains is shown in Fig. 1(b). This analysis indicates a homogeneous distribution of all the elements throughout the grains.

The samples of an appropriate size were prepared for the dielectric and pyroelectric measurements. The cut and polished samples were coated with silver electrodes, using an appropriate silver paste, without thermal treatment.

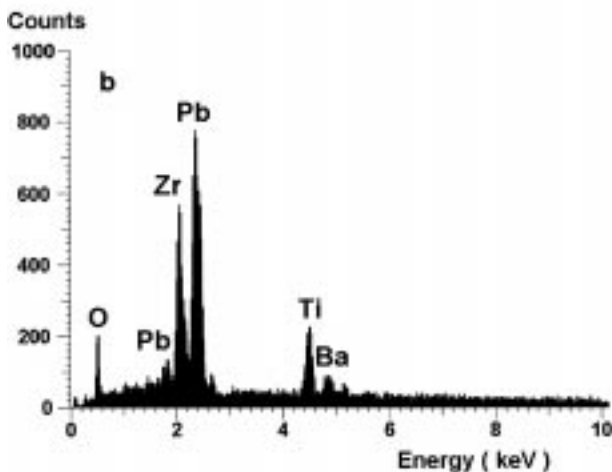
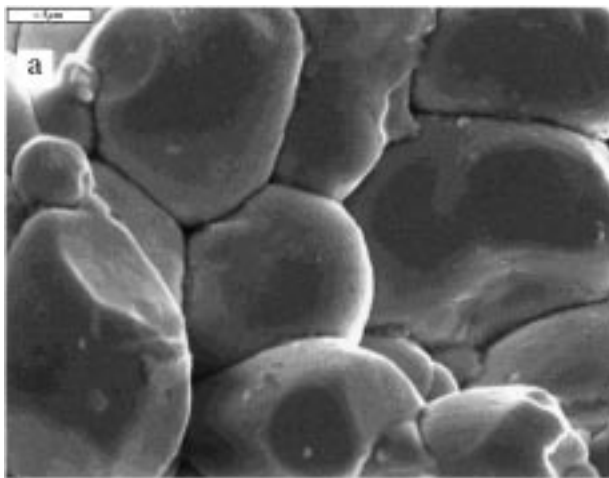


Fig. 1. Scanning electron micrograph of fracture surface of (a) investigated ceramics and (b) the EDS analysis obtained for one of the grains.

3 Dielectric Measurements

The samples of 0.6 mm thickness were used for the measurements of dielectric constant and loss factor as a function of temperature. These measurements were performed at eleven various frequencies of the measuring electric field, using a computerized automatic measuring system. They were carried out in successive heating-cooling cycles at the constant rate of temperature changes equal 2°C min⁻¹.

The examples of $\varepsilon(T)$ and $\tan \delta(T)$ curves, for the first and second heating process, are shown in Fig. 2. The virgin sample was used in the first heating-cooling cycle. The sample was rejuvenated in this way. As shown (Fig. 2) the ε and $\tan \delta$ as a function of temperature are changed considerably after this process. This concerns in particular the high frequency dielectric characteristics. The $\varepsilon(T)$ and $\tan \delta(T)$ curves are similar for the second and the following heating-cooling cycles. These curves, obtained on cooling, show only the normal, relatively small thermal hysteresis effect. Broad maxima in the $\varepsilon(T)$ curves occur at temperatures of diffuse FE-PE phase transitions T_m , which increase with the frequency of the measuring field (Fig. 3). The values of ε_{\max} decrease with increase in frequency. The changes of the ε_{\max} and T_m , caused by the rejuvenation, are considerably higher in the range of higher frequencies. At temperatures $T \gtrsim 290^\circ\text{C}$, i.e. in the PE phase, the additional strongly broadened maxima arise in the $\varepsilon(T)$ curves. They are more distinct for lower frequency and gradually disappear when the frequency is in excess of about 10^4 Hz. These maxima are separated from the ε_{\max} at T_m by local minima in the $\varepsilon(T)$ curves. The ε_{\min} and the corresponding temperatures differ also for the virgin and rejuvenated states of the sample.

The loss factor also strongly depends on the frequency of the measuring electric field. Only in case of the lowest frequency of this field (i.e. 10^2 Hz), the temperatures corresponding to ε_{\max} and $(\tan \delta)_{\min}$ are fairly consistent. In case of higher frequencies the local minima in the $\tan \delta(T)$ curves occur at temperatures higher than T_m , contrary to the behaviour in normal ferroelectrics. The diagram of natural logarithm of the measuring frequency versus the reciprocal absolute temperature, at which the minima in the $\tan \delta(T)$ and $\varepsilon(T)$ curves occur, is shown in Fig. 4 for the second heating [Fig. 2(b) and (c)]. Linear character of these dependences proves that the process responsible for the increase of ε and $\tan \delta$ at temperatures higher than the one corresponding to their local minima, can be described by formula $f = f_0 \exp(-E_a/kT_{\min})$ with activation energy $E_a = 1.5$ eV. The data obtained

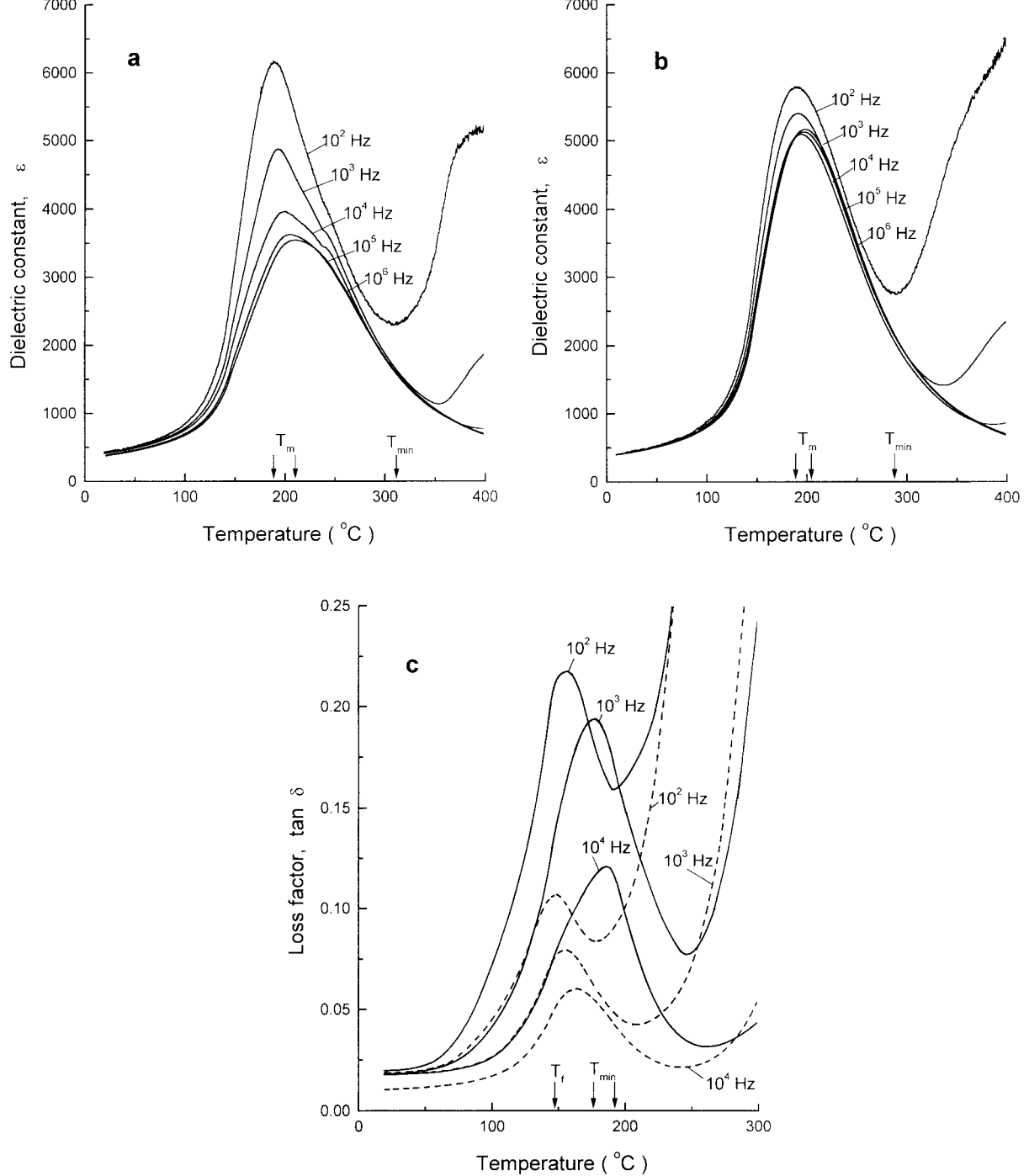


Fig. 2. Dielectric constant as a function of temperature, measured at various frequencies of the measuring field on (a) the first and (b) the second heating processes and (c) the loss factor versus temperature for the first (solid lines) and the second (dashed lines) heating for chosen frequencies.

for the virgin sample show bigger scatter in relation to the strength lines shown in Fig. 4. In this case the values of ϵ and $\tan \delta$ vary not only with temperature but also with time at constant temperature because the rejuvenation process is, namely, dependent on these two factors.

The temperature dependence of the remanent polarization (P_r) was determined from the hysteresis loop measurements for the previously rejuvenated sample. These measurements were carried out in a field of frequency 50 Hz and strength 10 kV cm^{-1} . The dependences of P_r and coercive field

E_C on temperature are shown in Fig. 5. The course of the $P_r(T)$ curve differ markedly from that observed in the normal ferroelectrics with first order FE-PE phase transition. It especially concerns the surroundings of this phase transition and the temperature range below 100°C . On heating P_r first increases up to about 100°C and then starts to decrease approximately linearly at about 145°C . The $P_r(T)$ curve behaviour in the range from about 145°C up to T_m and especially the gradual change of the hysteresis loops to the slim one, as well as additional data shown below, prove that

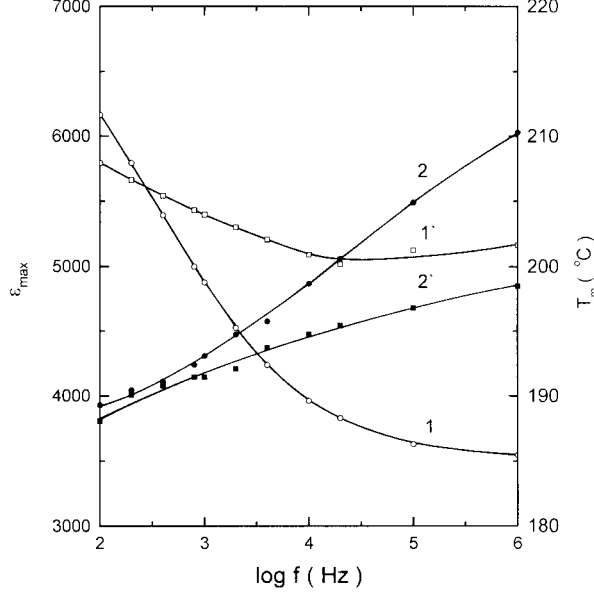


Fig. 3. The maxima in $\varepsilon(T)$ curves and corresponding temperatures T_m as a function of frequency of measuring field for the first (curves 1 and 2) and the second (curves 1' and 2') heating.

the temperature $\sim 145^\circ\text{C}$ can be identified with the freezing temperature (T_f), characteristic for the relaxor ferroelectrics. A relatively steeper change of the P_r takes place in the vicinity of T_m .

4 The Pyroelectric and Thermally Stimulated Depolarization Currents

As proved in our earlier paper,⁷ reporting on investigations of PLZT ceramics, the observed

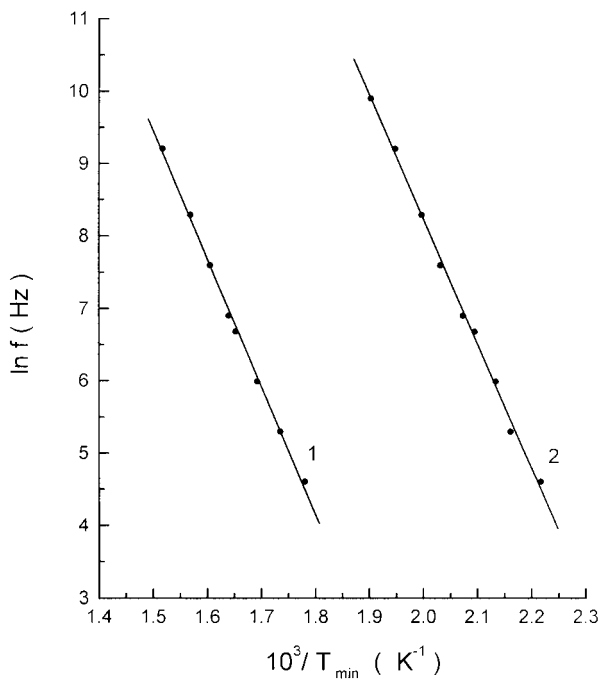


Fig. 4. Natural logarithm of the measuring frequency versus the reciprocal absolute temperatures at which the minima in (1) the $\varepsilon(T)$ and (2) $\tan \delta(T)$ curves occur.

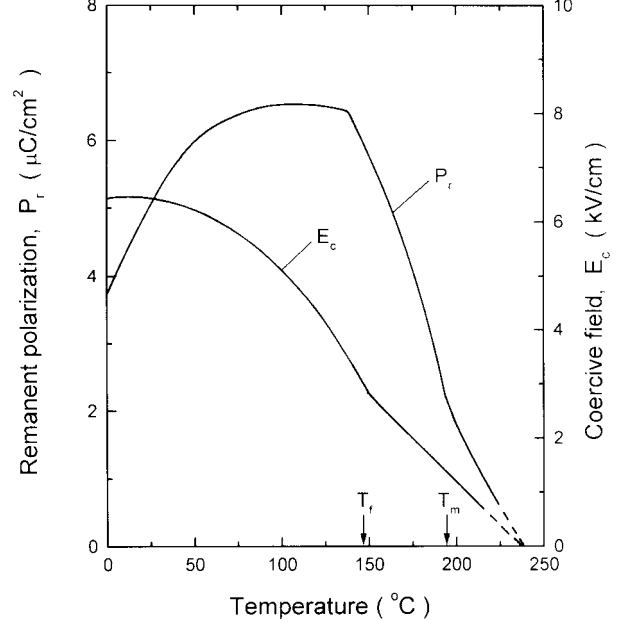


Fig. 5. The remanent polarization and coercive field as a function of temperature, obtained from hysteresis loop measurements.

low-frequency dielectric dispersion is connected with a space-charge polarization formed by orientation of the polar microregions, separation of mobile ion defects and with its interaction with the spontaneous polarization of ferroelectric material. These two kinds of polarization can be investigated by measurements of pyroelectric and thermally stimulated depolarization currents. To carry out these measurements the rejuvenated sample (at 430°C for 10 min) was first polarized by d.c. electric field (E_p) for 10 min, at temperatures (T_p) selected from the FE and PE phases ranges, and during subsequent cooling to room temperature under the field. After discharging by short-circuiting the sample was heated with a rate of 5°C min^{-1} , through the FF-PE phase transition up to about 400°C , when it was fully depolarized. Pyroelectric and thermally stimulated depolarization (TSDC) currents were recorded numerically as a function of temperature and time during heating. Such procedures of pre-polarization and depolarization were repeated successively for different conditions and in particular for the polarizing field of various strength from the range $E_p = 1\text{--}6\text{ kV cm}^{-1}$, applied at constant temperature and, for the various temperatures, when the field of a constant strength was applied. The current recorded during each heating stage allows to draw a graph of the current versus temperature or time which is presented below.

The $J(T)$ curves shown in Fig. 6 were obtained when the pre-polarization was carried out by means of a constant electric field of strength $E_p = 1\text{ kV cm}^{-1}$ at temperatures T_p taken from the range $100\text{--}225^\circ\text{C}$, i.e. the range surrounding the

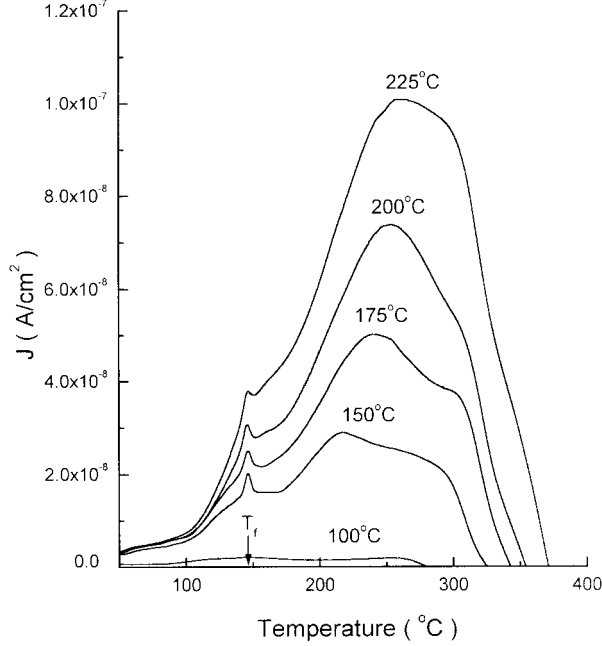


Fig. 6. The pyroelectric and thermally stimulated depolarization currents versus temperature, for the samples pre-polarized by applying constant electric field of strength $E_p = 1 \text{ kV cm}^{-1}$ at various temperatures shown in the figure.

temperature range $T_f - T_m$ (see Fig. 5). In the case of $T_p < T_f$, the relatively small current ($J < 2 \times 10^{-9} \text{ A cm}^{-2}$) shows a broad maximum in the vicinity of T_f and another broad maximum in the range of PE phase. In the case of higher temperatures $T_p > T_f$, a much greater current ($10^{-8} - 10^{-7} \text{ A cm}^{-2}$) shows distinct peaks of pyroelectric current, corresponding to the beginning of the P_r decrease in vicinity of T_f (see Fig. 5) and the broad maxima at higher temperatures from the range $\sim 215 - 250^\circ\text{C}$ (PE phase). The last-mentioned maxima in the depolarization current versus temperature curve occur in any case at temperatures higher than the T_p at which the sample was pre-poled. The current decreases above this temperature range, first slowly, then-rapidly. It is noteworthy that this steep fall of the current starts at about 300°C i.e. at a temperature corresponding to the one at which ε_{\min} occurs for 10^2 Hz [see Fig. 2(a) and (b)]. The integrated pyroelectric current (J_p versus time) corresponds to only a small change of a spontaneous polarization ($\Delta P_s \cong 0.3 \mu\text{C cm}^{-2}$) while the integrated TSDC gives large values of space charge polarization $P_{s,\text{ch}} \cong 55 - 196 \mu\text{C cm}^{-2}$ for T_p from 150 to 225°C , respectively. The temperature dependence of pyroelectric and TSD currents, for the sample polarized by applying electric field of strength $E_p = 1, 2, 4,$ and 6 kV cm^{-1} at $T_p = 100^\circ\text{C}$, is shown in Fig. 7. The peaks of pyroelectric current occur in a vicinity of the freezing temperature T_f . The maxima in the TSD current occur at temperatures from the range $250 - 270^\circ\text{C}$. The dependences of the maximal

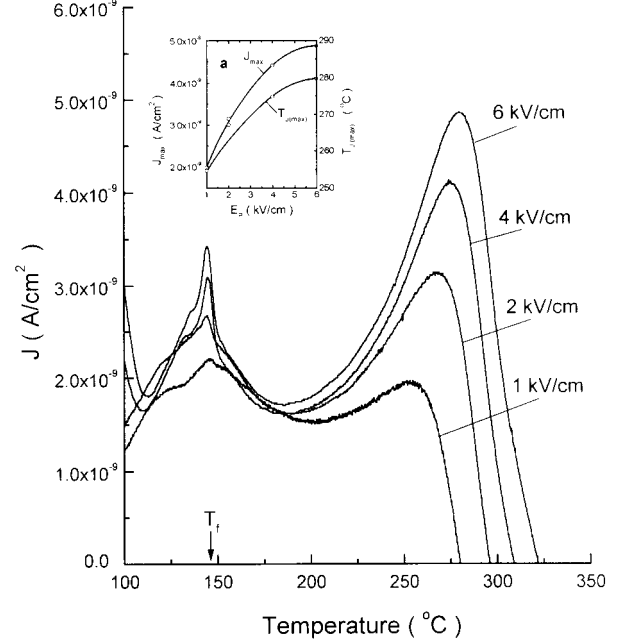


Fig. 7. The pyroelectric and thermally stimulated depolarization currents versus temperature, for the sample pre-polarized by applying electric field of various strength E_p (shown in the figure) at constant temperature $T_p = 100^\circ\text{C}$. Maxima in the $J(T)$ curves and corresponding temperatures as a function of strength of the polarizing field are shown in the inserted figure (a).

values of TSDC (J_{\max}) and temperatures at which these maxima occur in the PE phase ($T_{J_{\max}}$) are shown as a function of strength of polarizing electric field in the inserted Fig. 7(a). Noteworthy are the symptoms of saturation in the $J_{\max}(T)$ curve.

5 Discussion

The reported experimental data prove the behaviour of the investigated PBZT ceramics as relaxor ferroelectric, which was already suggested and proved by Li and Haertling for the Bi_2O_3 doped PBZT ceramics.² The ceramics studied show the features well known for relaxor ferroelectrics such as: reducing ε_{\max} and shift of the corresponding temperature T_m with increasing frequency; shift of the minima in the $\tan \delta(T)$ curves to temperatures $T > T_m$; transformation of normal hysteresis loops to the slim shaped form above the freezing temperature T_f ; an occurrence of pyroelectric peak in the vicinity of this temperature, etc. It is commonly believed that the relaxor behaviour originates from diffuse character of the FE-PE phase transition, caused by compositional fluctuations (e.g. local differences in the Pb/Ba and Zr/Ti ratios in case of the PBZT ceramics) and by defects of different kinds (for instance-vacancies in the Pb and O sublattices). The microregions of varying composition or concentration of defects have different local FE-PE transition temperatures. A size distribution of these microregions gives rise to a

dielectric dispersion—a feature characteristic of the most typical relaxor ferroelectrics.^{8–11} As known, the mobile ion defects, responsible for the ageing process, recombine partially and reach random distribution during the rejuvenation process. These processes help to understand the observed changes in the characteristics of the virgin and rejuvenated states of the sample. The mechanical strains were also removed in this process.

Evident correlation was ascertained between the temperature variations in the dielectric properties (ϵ , $\tan \delta$ and P_r) on the one hand and the temperature changes of pyroelectric and thermally stimulated depolarization currents on the other hand. Similar correlation in these characteristics, observed by us in some PLZT-type ceramics was interpreted in our previous paper⁷ basing on the papers^{8–11} cited above and many others related to relaxor ferroelectrics. This qualitative interpretation model can be utilized for a more detail discussion of the results, reported in the present paper.

Some remaining FE domains (clusters) can be surrounded by the PE phase in the temperature range $T_f < T < T_m$ and in a certain range of $T > T_m$ due to the above-mentioned differentiation in the local Curie temperatures. The depolarization field associated with P_s of such domains tends to the compensated state by two possible ways, known from macroscopic considerations. One of them consists in the formation of a locally compensated polydomain structure (for instance by formation of twin domains). The new smaller domains have different Curie temperatures due to the local electric and mechanical strains. So, this process plays a role in serving the remaining FE domains in small microdomains of nanometer size that give rise to relaxor behaviour and in particular to a quick response and high frequency dielectric dispersion. The second way consists of the P_s screening by electron and ion space charges from the surrounding medium. Such compensated FE domains are also stabilized in this manner at much higher temperatures above T_m . Even after the disappearance of P_s inside the screened FE domains at a high enough temperature, the nonredomly distributed space charges (previously participating in the screening process) and the associated polar microregions remain in the PE matrix because of the relatively low mobility of ion defects and the long relaxation time. It is reasonable to believe that these polar microregions are responsible for the observed broad maxima in the $\epsilon(T)$ curves in the specified range of PE phase. At lower temperatures from this range their dipole moments are more or less compensated by electron-hole carriers. They are also stabilized in this way in a certain temperature range, especially in the surface layers,

where electron carriers injected from the electrodes play an important role. At high enough temperatures the electron release, owing to thermal generation, causes an appearance or an increase of the resultant dipole moment of these microregions, giving rise to the observed increase of ϵ in the low frequency range. The liberated electron carriers increase also the $\tan \delta(T)$ values. This tentative interpretation is strongly supported by the fact that the crosscorrelation between the temperatures at which the $\epsilon(T)$ and $\tan \delta(T)$ curves show the local minima and start to increase, obeys the same formula $f = f_0 \exp(-E_a/kT_{\min})$ (Fig. 4) with the same activation energy $E_a = 1.5$ eV.

The mutual compensation of the polarization component resulting from the orientation of polar microregions by the electronic and ionic space charges, together with the carriers injected from the electrodes, cause the observed shift of the maxima in TSDC towards temperatures higher than the ones at which the sample was pre-polarized (Fig. 6). The thermally stimulated depolarization current has a complex character, which consists of components associated with disorientation process of the polar microregions and migration of released ion and electron carriers under the bias internal electric field and gradients of concentration. A more detailed description of these processes is given in monography.¹²

6 Conclusions

1. The investigated $(\text{Pb}_{0.75}\text{Ba}_{0.25})(\text{Zr}_{0.70}\text{Ti}_{0.30})\text{O}_3$ ceramics show properties typical for relaxor ferroelectrics.
2. Correlation between the temperature variations in the dielectric properties on one hand and the pyroelectric and thermally stimulated depolarization currents on the other was ascertained.
3. Activation character of processes responsible for the observed anomaly in dielectric and depolarization characteristics was proved.

References

1. Ikeda, T., Studies in $(\text{Ba,Pb})(\text{Zr,Ti})\text{O}_3$ system. *J. Phys. Soc. Jpn*, 1959, **14**, 168.
2. Li, G. and Haertling, G., Dielectric, ferroelectric and electric field-induced strain properties of $(\text{Pb}_{1-x}\text{Ba}_x)(\text{Zr}_{1-y}\text{Ti}_y)\text{O}_3$ ceramics. *Ferroelectrics*, 1995, **166**, 31.
3. Gundel, H. Riege, H. Wilson, E. J. N. Hańderek J. and Zioutas, K., Copious electron emission from PLZT ceramics with a high zirconium concentration. *Ferroelectrics*, 1989, **100**, 1.
4. Gundel, H. Hańderek, J. Riege, H. Wilson E. J. N. and Zioutas, K. Pulsed electron emission from PLZT ceramics. *Ferroelectrics*, 1990, **109**, 137; 1993, **110**, 183.
5. Gundel, H. Hańderek J. and Riege, H., Time-dependent electron emission from ferroelectrics by external pulsed electric field. *J. Appl. Phys.*, 1991, **69**, 975.

6. Kanai, H., Furukawa, O., Abe, H. and Yamashita, Y., Dielectric properties of $(\text{Pb}_{1-x}\text{X}_x)(\text{Zr}_{0.7}\text{Ti}_{0.3})\text{O}_3$ (X = Ca, Sr, Ba) ceramics. *J. Am. Ceram. Soc.*, 1994, **77**, 2620.
7. Hańderek, J., Ujma, Z., Carabatos-Nedelec, C., Kugel, G. E., Dmytrów, D. and Harrad, I. El., Dielectric, pyroelectric and thermally stimulated depolarization current investigations on lead-lanthanum zirconate-titanate $x/95/5$ ceramics with La content $x=0.5\%–4\%$. *J. Appl. Phys.*, 1993, **73**(1), 367.
8. Cross, L. E., Relaxor ferroelectrics. *Ferroelectrics*, 1997, **76**, 241.
9. Hilton, A. D. Randall, C. A. Barber, D. J. and Strout, T. R., TEM studies of $\text{Pb}(\text{Mg}_{1/3}\text{Nb}_{2/3})\text{O}_3\text{–PbTiO}_3$ ferroelectrics relaxors. *Ferroelectrics*, 1989, **93**, 379.
10. Pan, W. Y., Jiang, Q. V. and Cross, L. E., Aging effects in lead magnesium niobate type of relaxor ferroelectric ceramics. *Ferroelectrics*, 1989, **93**, 393.
11. ShROUT, T. R. Huebner, W. Randall, C. A. and Hilton, A. D., Eging mechanism in $\text{Pb}(\text{Mg}_{1/3}\text{Nb}_{2/3})\text{O}_3$ based relaxor ferroelectrics. *Ferroelectrics*, 1989, **93**, 361.
12. Brownlich, P. (ed.), Thermally stimulated relaxations in solids. *Topics in Applied Physics*, Vol. 37. Springer-Verlag, Berlin, Heidenberg, New York, 1997.